frontiers in Chemistry

ORIGINAL RESEARCH
published: 15 April 2020
doi: 10.3389/fchem.2020.00293

Effect of $CeH_{2.73}$-CeO_2 Composites on the Desorption Properties of Mg_2NiH_4

*Kaiyao Wu, Daqian Cai, Kaimei Shao, Tuguang Xue, Peng Zhang, Wei Li and Huai-Jun Lin**

Institute of Advanced Wear and Corrosion Resistant and Functional Materials, Jinan University, Guangzhou, China

A series of $CeH_{2.}73/CeO_2$ composites with different ratios of hydride and oxide phases are prepared from the pure cerium hydride via oxidation treatments in the air at room temperature, and they are subsequently doped into Mg_2NiH_4 by ball milling. The desorption properties of the as-prepared Mg_2NiH_4+$CeH_{2.73}/CeO_2$ composites are studied by thermogravimetry and differential scanning calorimetery. Microstructures are studied by scanning electron microscopy and transmission electron microscopy, and the phase transitions during dehydrogenation are analyzed through *in situ* X-ray diffraction. Results show that the initial dehydrogenation temperature and activation energy of Mg_2NiH_4 are maximally reduced by doping the $CeH_{2.73}/CeO_2$ composite with the same molar ratio of cerium hydride and oxide. In this case, the $CeH_{2.73}/CeO_2$ composite has the largest density of interface among them, and the hydrogen release effect at the interface between cerium hydride and oxide plays an efficient catalytic role in enhancing the hydrogen desorption properties of Mg_2NiH_4.

Keywords: Hydrogen storage materials, dehydrogenation, Mg_2NiH_4, $CeH_{2.73}/CeO_2$, catalysts

OPEN ACCESS

Edited by:
Yongfeng Liu,
Zhejiang University, China

Reviewed by:
Yao Zhang,
Southeast University, China
Rapee Utke,
Suranaree University of Technology, Thailand

***Correspondence:**
Huai-Jun Lin
hjlin@jnu.edu.cn

Specialty section:
This article was submitted to Inorganic Chemistry, a section of the journal Frontiers in Chemistry

Received: *22 February 2020*
Accepted: *24 March 2020*
Published: *15 April 2020*

Citation:
Wu K, Cai D, Shao K, Xue T, Zhang P, Li W and Lin H-J (2020) Effect of $CeH_{2.73}$-CeO_2 Composites on the Desorption Properties of Mg_2NiH_4. Front. Chem. 8:293. doi: 10.3389/fchem.2020.00293

INTRODUCTION

With the advantages of abundant natural resources and no pollution to the environment, hydrogen has been widely considered as an ideal carbon-free energy carrier. Hydrogen energy storage technology is a prerequisite for the large-scale utilization of hydrogen energy. Light-weight solid-state hydrogen storage materials have been considered to be ideal candidates for hydrogen storage because of the high hydrogen storage density and security consideration (Mohtadi and Orimo, 2016; Wang et al., 2016). Among the existing solid-state hydrogen storage materials, Mg-based hydrogen storage materials are widely studied and considered as promising solid-state hydrogen storage materials due to the high hydrogen storage capacity, abundance on the earth and low production cost (Ouyang et al., 2013, 2017; Rusman and Dahari, 2016; Shao et al., 2018).

MgH_2 and Mg_2NiH_4 are two typical Mg-based hydrogen storage materials with hydrogen densities of 7.6 wt and 3.6 wt%, respectively (Reilly and Wiswall, 1968; Bogdanović, 1984; Liu et al., 2016, 2019; Zhan et al., 2016; Chen et al., 2018; Ding et al., 2019). Nevertheless, the stable thermodynamics and slow kinetics of hydrogen storage properties of Mg-based materials lead to harsh conditions for dehydrogenation (Bogdanović et al., 2010; Jain et al., 2010). The hydrogen desorption temperatures of MgH_2 and Mg_2NiH_4 are usually as high as 250–350C. Many efforts have been made by researchers to improve the kinetics and reduce the desorption temperatures of MgH_2 and Mg_2NiH_4. The commonly conducted methods include mechanical alloying, doping catalysts, nanostructuring, surface modification and so on (Terashita et al., 1999; Lin et al., 2012a, 2016; Shao et al., 2012; Eleskandarany et al., 2016; Zhang et al., 2017; Khan et al., 2018; Xu et al., 2019).

Doping catalysts by ball milling is a commonly-used and efficient method to enhance the hydrogenation/dehydrogenation kinetics of Mg-based materials (Ouyang et al., 2014a,b; Wang and Wang, 2017). To date, many additives have been explored, including oxides (Barkhordarian et al., 2003), transition metals (Hanada et al., 2005), hydrides (Ma et al., 2017), carbon-based materials (Lototskyy et al., 2013) and so on. It has been demonstrated that compounds with higher valences show higher catalytic effect on the hydrogen storage performances of Mg-based materials than that of the lower valence compounds (Bobet et al., 2002). Because of the unique 4*f* electron of the Ce element, Ce-based compounds are widely used in the catalysis field (Trovarelli, 1996). Long et al. (2013) reported Mg-Ce oxide powders produced by an arc plasma evaporation method. As a result, enthalpies of hydrogenation and dehydrogenation for Mg/MgH_2 reduce to −71.0 and 75.4 kJ/mol H_2, respectively. Moreover, the hydrogenation activation energy is reduced to only 47.75 kJ/mol. The composite can absorb 4.07 wt%-H at 323 K in 10 h. Their study indicates that minor addition of Ce oxide can remarkably improve the hydrogenation kinetics of Mg/MgH_2. We previously reported that CeF_4 was an efficient catalyst to enhance the hydrogen storage properties of MgH_2 (Lin et al., 2015), which can lead to reduced dehydrogenation temperature and activation energy because of the formation of new Mg-Ce-F species on the surface of MgH_2. Gulicovski (Gulicovski et al., 2012) et al. prepared MgH_2-CeO_2 composite by ball milling of MgH_2 and nano-CeO_2 particles. The dehydrogenation activation energy is reduced to 60 ± 10 kJ/mol, indicating that the activation energy is sufficiently decreased by the catalytic effect of vacant CeO_2 particles. We also developed a new symbiotic $CeH_{2.73}/CeO_2$ nano-catalyst, which was *in-situ* produced by controlling hydrogenation and oxidation treatments upon the amorphous Mg-Ce-Ni alloys (Lin et al., 2014), leading to significantly improved dehydrogenation performance of MgH_2-based composite. Moreover, *in situ* TEM and DFT study show that the remarkable catalysis effect is attributed to the spontaneous hydrogen release effect at the interface between cerium oxide and hydride. Because the composite contains only major MgH_2 but also minor Mg_2NiH_4, the effect of $CeH_{2.73}/CeO_2$ composite on the dehydrogenation properties of Mg_2NiH_4 has not been well-understood.

In order to clarify the effect of cerium hydride/oxide composites on the dehydrogenation properties of Mg_2NiH_4, in the present study, a series of $CeH_{2.73}/CeO_2$ composites with different ratios of cerium oxide and hydride were synthesized from pure cerium hydride via controlled oxidation treatments in the air at room temperature, and then they were doped into Mg_2NiH_4 by ball milling. The dehydrogenation properties of cerium hydride and cerium oxide-doped Mg_2NiH_4 were studied, and the initial dehydrogenation temperature and activation energy were characterized by TG-DSC and a Kissinger's method. Moreover, the phase transitions during dehydrogenation were analyzed through *in situ* XRD experiments.

EXPERIMENTAL DETAILS

Materials

The Mg_2NiH_4 used in this experiment was prepared by a method of hydrogenation combustion synthesis method (HCS), which was carried out in Prof. Yunfeng Zhu's group in Nanjing Tech University (Gu et al., 2009; Zhu et al., 2017). $CeH_{2.73}$ (purity >99%) was purchased from Hunan Research Institute of Non-ferrous metals. About 0.1 g $CeH_{2.73}$ powder was located in a plastic bottle of 3 ml, in the Ar glove-box. Then it was transferred into the small side box of glove-box. The door of side box was then open to let air in for different time: 0.5, 1.5, 3, 10, and 60 min. The oxidized $CeH_{2.73}$ became $CeH_{2.73}/CeO_2$ composites, and 2 mol% of $CeH_{2.73}/CeO_2$ composites were then doped into Mg_2NiH_4 by ball milling at 400 rpm for 4 h.

Characterizations

The phase structures were analyzed by X-ray diffraction (XRD), and the phase transition during dehydrogenation was analyzed by *in situ* XRD analysis. The XRD analysis was carried out by an X-ray diffractometer apparatus (UItima IV, Rigaku, Japan) with Cu-K α (λ = 0.15405 nm). The tube voltage and tube current were 40 kV and 40 mA, respectively. Thermogravimetry (TG) and Differential Scanning Calorimetery (DSC) were used to study the hydrogen desorption behaviors at different heating rates on a METTLER TGA/DSC 3^+ synchronous thermal analyzer. The microstructures of the Mg_2NiH_4-$Ce_{2.73}/CeO_2$ composites were observed by backscattered electron imaging using scanning electron microscope (SEM) and transition electronic microscopy (TEM).

RESULTS AND DISCUSSION

Preparation of the $CeH_{2.73}/CeO_2$ Catalysts

Six sets of $CeH_{2.73}/CeO_2$ composites prepared by oxidation treatments for different durations were analyzed by XRD. The $CeH_{2.73}/CeO_2$ composites are marked as S1, S2, S3, S4, S5, and S6, according to the oxidation duration of $CeH_{2.73}$ of 0, 0.5, 1.5, 3, 10, and 60 min, respectively. The diffraction patterns are shown in **Figure 1**. With the increase of oxidation time, $CeH_{2.73}$ gradually transforms into CeO_2. After oxidation of 60 min, no $CeH_{2.73}$ has left. The obtained XRD patterns were refined by a Jade 6.0 software and the phase contents were calculated by the K value (RIR) method. The relative contents of the CeO_2 phase as increase of the oxidation time are shown in **Figure 2**. The oxidation data can be fitted by the Avrami–Erofeev equation deduced from the nucleation and growth process:

$$\alpha = 1 - exp(-Bt^m), \quad (1)$$

where α is the ratio of reacted material to total material, m and B are constants. The fitted m is 1.085, which is very close to 1.07, indicating the oxidation of $CeH_{2.73}$ at room temperature is a three-dimensional interface reaction process (Lin et al., 2012b). For the S4 sample, the relative content of $CeH_{2.73}$ is 54.2 wt%, and the relative content of CeO_2 phase is 45.8 wt%, indicating almost

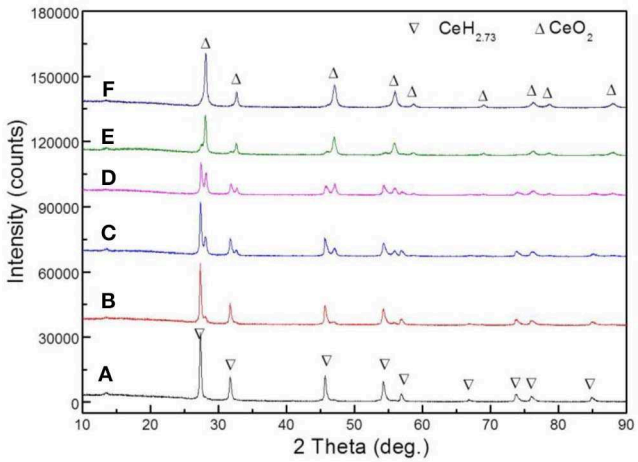

FIGURE 1 | XRD images of six groups of $CeH_{2.73}/CeO_2$ composite catalysts obtained by oxidation of $CeH_{2.73}$ for different durations: **(A)** 0 min, S1, **(B)** 0.5 min, S2, **(C)** 1.5 min, S3, **(D)** 3 min, S4, **(E)** 10 min, S5, **(F)** 60 min, S6.

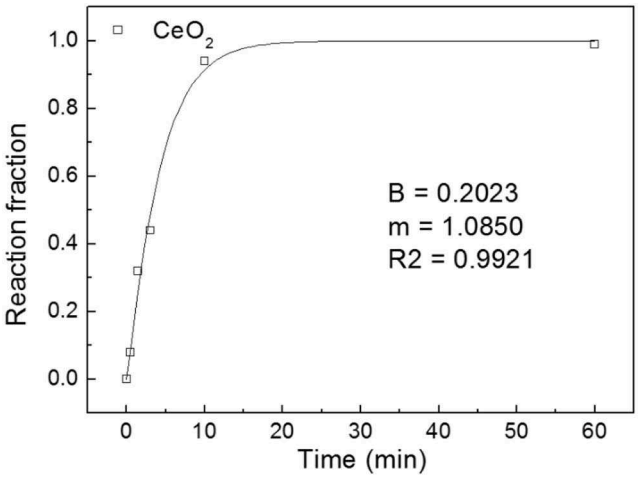

FIGURE 2 | Relative content of the CeO_2 composites phase as increase of oxidation time.

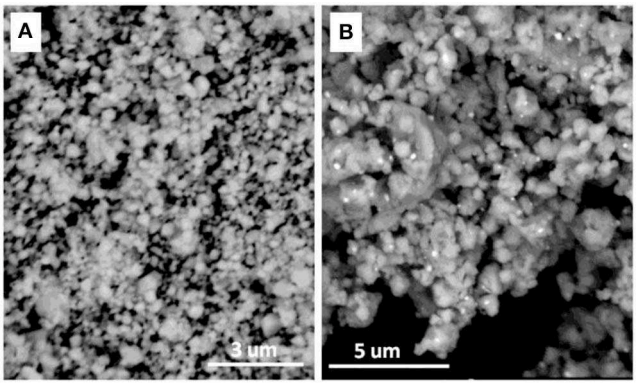

FIGURE 3 | BSEM image of **(A)** the as-oxidized $CeH_{2.73}/CeO_2$ composite (S5) and **(B)** the ball-milled Mg_2NiH_4 + S5 sample.

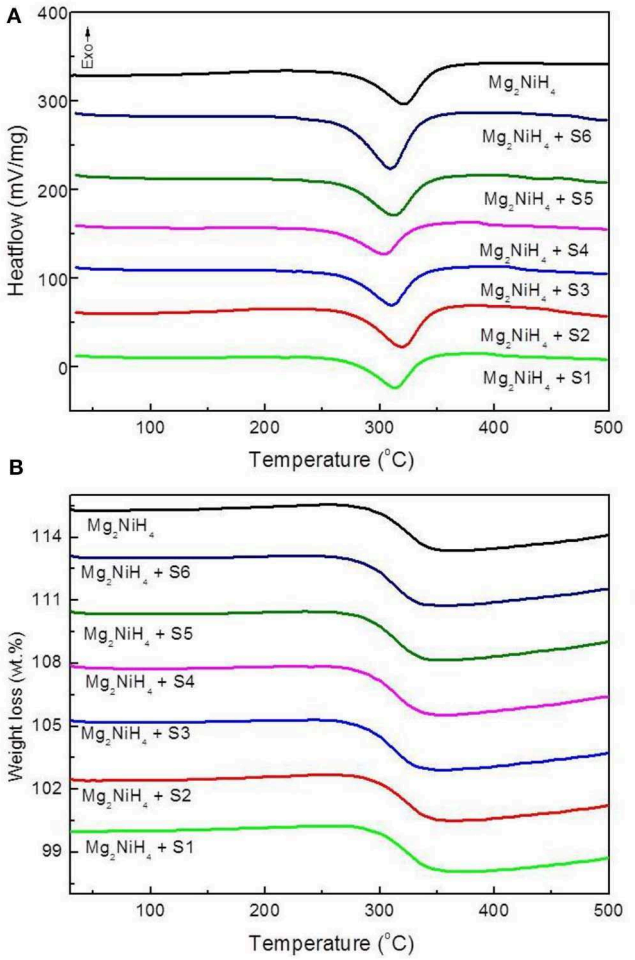

FIGURE 4 | (A) DSC and **(B)** TG curves of the ball-milled Mg_2NiH_4-$CeH_{2.73}/CeO_2$ composites materials, at a heating rate of 20 K/min.

the same molar ratio of cerium hydride and oxide when the oxidation time is around 3 min. After the oxidation treatments, the samples were doped into Mg_2NiH_4 by ball milling.

In order to understand the morphologies of the $CeH_{2.73}/CeO_2$ composite doped Mg_2NiH_4, back scattering scanning electron microscopy (BSEM) was carried out. Because the S1–S4 sample will continue to oxidize in the air, the S5 doped Mg_2NiH_4 sample was selected as the experimental material. The morphologies of the as-prepared $CeH_{2.73}/CeO_2$ composite (S5 sample) and the ball-milled Mg_2NiH_4 + S5 sample are shown in **Figure 3**. It could be clearly seen that the particle size of the as-prepared $CeH_{2.73}/CeO_2$ composite is about 200–400 nm. After ball milling, the particle size of the $CeH_{2.73}/CeO_2$ composite is greatly reduced to below 30–100 nm. **Figure 3B** shows that the $CeH_{2.73}/CeO_2$ composites, which are brighter particles, are uniformly distributed in the Mg_2NiH_4 matrix. The homogeneous $CeH_{2.73}/CeO_2$ composites could be beneficial for catalyzing

hydrogen storage properties for the Mg-based materials (Hong et al., 2009; Shao et al., 2011; Li et al., 2018).

Dehydrogenation of Mg_2NiH_4 + $CeH_{2.73}/CeO_2$ Composites

The decomposition behaviors of the ball-milled Mg_2NiH_4+$CeH_{2.73}/CeO_2$ composites are studied by TG-DSC synchronous thermal analyzer as shown in **Figure 4**. The DSC study of Mg_2NiH_4 + $CeH_{2.73}/CeO_2$ composites are at a heating rate of 20 K/min, showing the dehydrogenation initial temperature of Mg_2NiH_4 decreases after addition of $CeH_{2.73}/CeO_2$ composites. Among the six sets of catalysts, the S4 sample obtained by oxidation of $CeH_{2.73}$ for 3 min, exhibits the highest catalytic effect on reducing the dehydrogenation temperature of Mg_2NiH_4. The dehydrogenation temperature is decreased to 267°C, which is about 17°C lower than the that of as-milled Mg_2NiH_4 (284°C).

To further elucidate the dehydrogenation activation energy of the Mg_2NiH_4-$CeH_{2.73}/CeO_2$ composites, DSC experiments for the Mg_2NiH_4 + $CeH_{2.73}/CeO_2$ composites at heating rates of 10 K/min and 50 K/min were carried out (results not shown). The activation energy of the dehydrogenation process was calculated by using the Kissinger's method (Kissinger, 1957),

$$\ln\left(\frac{\beta}{T_m^2}\right) = \frac{E_{ds}}{RT_m} + C \quad (2)$$

where E_{des} is the dehydrogenation activation energy, T_m, β, R, and C are the peak temperature, heating rate of DSC experiments, gas constant and another constant, respectively. The relation between T_m and β is linearly fitted as plotted in **Figure 5**, and the activation energy was summarized in **Table 1**. Results show that the S4 sample by oxidation of $CeH_{2.73}$ for 3 min exhibits the best catalytic effect on reducing the dehydrogenation activation energy of Mg_2NiH_4 (from 76.3 kJ/mol to 62.6 kJ/mol). Zhang (Zhang et al., 2018) et al. suggested that alloying Mg_2Ni with Ti, V, Fe, or Si could reduce the hydrogenation and dehydrogenation activation energies to 60–70 kJ/mol. Our study suggests that the $CeH_{2.73}/CeO_2$ composites are also efficient to reduce the dehydrogenation activation energy of Mg_2NiH_4.

Combining XRD and TG-DSC study, it indicates clearly that the initial dehydrogenation temperature and activation energy of Mg_2NiH_4 are maximally reduced as the cerium hydride and cerium oxide are in the same amount. These results well-accord with our previous finding on the effect of $CeH_{2.73}/CeO_2$ composites on the dehydrogenation properties of MgH_2 (Lin et al., 2014), which means the $CeH_{2.73}/CeO_2$ composite with the same molar ratio of cerium hydride and oxide could be a good catalyst for the dehydrogenation properties of Mg-based hydrogen storage materials, including both MgH_2 and Mg_2NiH_4.

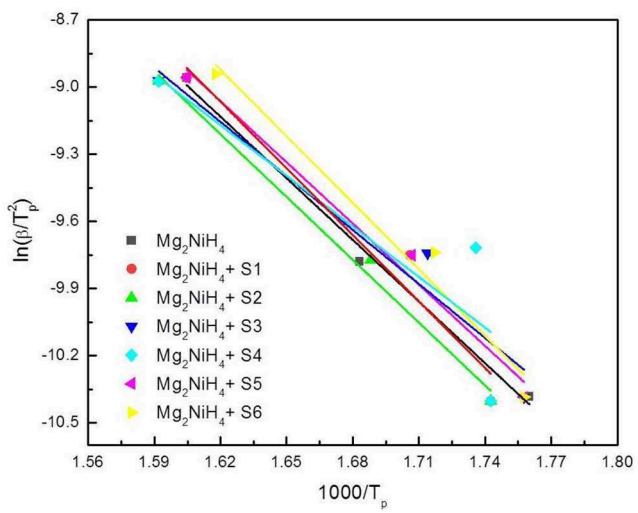

FIGURE 5 | Kissinger's Plot of Mg_2NiH_4-$CeH_{2.73}/CeO_2$ composite system.

TABLE 1 | Initial temperature, peak temperature and activation energy of dehydrogenation for the ball-milled Mg_2NiH_4 + $CeH_{2.73}/CeO_2$ composites (20 K/min).

Materials	Initial temperature (°C)	Peak temperature (°C)	Activation energy (kJ/mol)
Mg_2NiH_4	284	320	76.3
Mg_2NiH_4 + S1	283	317	82.4
Mg_2NiH_4+ S2	283	323	77.8
Mg_2NiH_4+ S3	276	315	66.9
Mg_2NiH_4+ S4	267	308	62.6
Mg_2NiH_4+ S5	276	317	75.7
Mg_2NiH_4+ S6	275	314	82.3

Microstructures of the Mg_2NiH_4 + $CeH_{2.73}/CeO_2$ Composite

The morphology and microstructure of Mg_2NiH_4 and as-oxidized 10 min $CeH_{2.73}/CeO_2$ composite (S5) are shown in **Figure 6a**. From the HRTEM images in **Figure 6b**, it could be found that the composite matrix is Mg_2NiH_4, which lattice fringe corresponds to the lattice plane of (111) and (220). Particle sizes of the CeO_2 nanoparticles are in a large range from 50–200 to 5–10 nm, which have been clearly shown in **Figures 6a,d**, respectively. Moreover, it could be seen that the *in-situ* generated CeO_2 particles are embedded homogeneously in the Mg_2NiH_4 matrix after ball milling. The interfaces between Mg_2NiH_4 and CeO_2 composite, as shown in **Figures 6c,d**, are contacted closely with each other. The homogeneously distributed catalysts can lead to high catalysis effect, and thus be beneficial for the hydrogenation/dehydrogenation properties of Mg_2NiH_4. Because of the too small amount of $CeH_{2.73}$, we could not clarify their microstructures in the TEM study.

In situ XRD of Dehydrogenation

The phase transition of the Mg_2NiH_4 + S5 sample during dehydrogenation was further studied by *in situ* XRD. The obtained *in situ* XRD patterns are shown in **Figure 7**. The XRD pattern of Mg_2NiH_4 + S5 sample at room temperature contains the diffraction peaks of Mg_2NiH_4 and CeO_2 because the XRD intensity of $CeH_{2.73}$ is too weak. The diffraction peaks of CeO_2 do not obviously change during the whole dehydrogenation

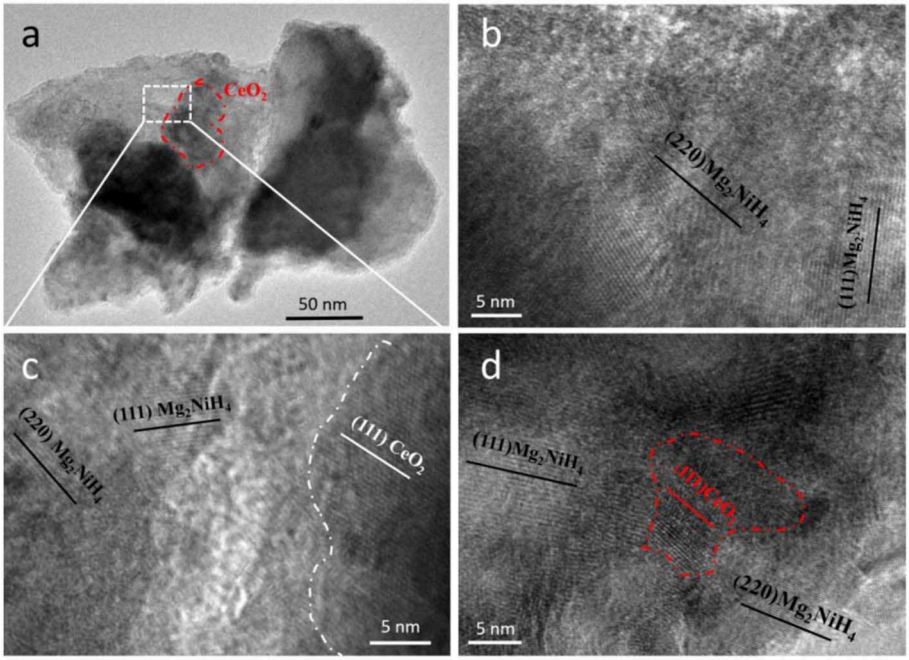

FIGURE 6 | (a) TEM and **(b–d)** HRTEM images of the Mg_2NiH_4 + S5 composite. **(b)** shows the Mg_2NiH_4 matrix, **(c)** shows the magnified interface between Mg_2NiH_4 and CeO_2, **(d)** shows a CeO_2 particle with size of 5–10 nm.

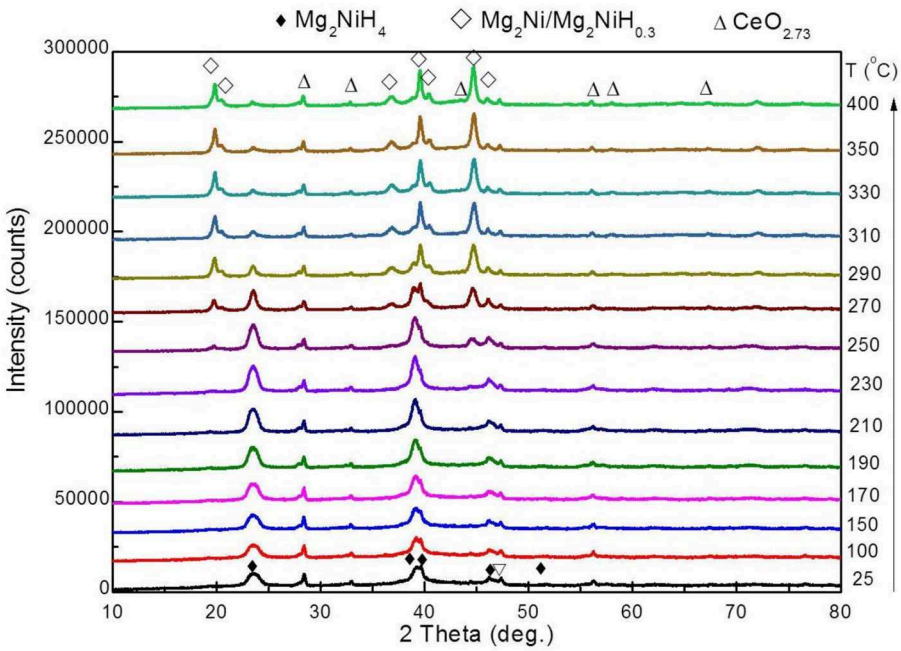

FIGURE 7 | *In situ* XRD patterns of dehydrogenation of the ball-milled Mg_2NiH_4 + S5.

process, indicating that the CeO_2 phase might act as a catalyst of Mg_2NiH_4 dehydrogenation. When the temperature was raised to 250°C, the diffraction peak of $Mg_2NiH_{0.3}/Mg_2Ni$ phase appears, which means the dehydrogenation of Mg_2NiH_4 starts. As temperature increases, the intensity of $Mg_2NiH_{0.3}/Mg_2Ni$ phase gradually enhances, and that of the Mg_2NiH_4 peaks decreases. As temperature reaches about 330°C, the diffraction peaks of CeO_2 remains unchanged and no MgO is found.

The *in situ* XRD patterns are then refined using Jade 6.0, and the relative contents of phases are calculated by the RIR method. At 270°C, the relative content of $Mg_2NiH_{0.3}$ phase is 47.1 wt%, and the relative content of Mg_2NiH_4 phase is 52.9 wt%. After heating to 290°C, the relative content of the two phases changes rapidly, and the relative content of $Mg_2NiH_{0.3}$ phase increases to 81.8 wt% and Mg_2NiH_4 The relative content of the phase was reduced to 18.2 wt%. Subsequently, the rate of phase change during the heating process was significantly slowed down. The relative content of $Mg_2NiH_{0.3}$ phase was 89.1 wt% at 400°C, and the relative content of Mg_2NiH_4 phase reduces to about 10.9 wt%.

CONCLUSION

In summary, $CeH_{2.73}/CeO_2$ composites with different proportions of cerium hydride and oxide are synthesized from pure cerium hydride via oxidation treatments in the air at room temperature. Oxidation time of 3 min leads to formation of $CeH_{2.73}/CeO_2$ composite with the same molar ratio of cerium hydride and oxide, which maximally reduces the initial dehydrogenation temperature and activation energy of Mg_2NiH_4. The $CeH_{2.73}/CeO_2$ composite with the same molar ratio is a good catalyst for reducing dehydrogenation temperatures of Mg-based materials.

DATA AVAILABILITY STATEMENT

The raw data supporting the conclusions of this article will be made available by the authors, without undue reservation, to any qualified researcher.

AUTHOR CONTRIBUTIONS

KW and DC: methodology and writing - original draft. KS and TX: methodology and formal analysis. PZ: resources and supervision. WL: supervision and project administration. H-JL: conceptualization, resources, writing - review and editing, supervision, and funding acquisition.

ACKNOWLEDGMENTS

We thank Prof. Yunfeng Zhu for providing the Mg_2NiH_4. Financial supports from National Natural Science Foundation of China (No. 51601090), Guangdong Basic and Applied Basic Research Foundation (No. 2019A1515011985) and the Fundamental Research Funds for the Central Universities (No. 21619415) are appreciated.

REFERENCES

Barkhordarian, G., Klassen, T., and Bormann, R. (2003). Fast hydrogen sorption kinetics of nanocrystalline Mg using Nb2O5 as catalyst. *Scr. Mater.* 49, 213–217. doi: 10.1016/S1359-6462(03)00259-8

Bobet, J. L., Chevalier, B., Song, M. Y., Darriet, B., and Etourneau, J. (2002). Hydrogen sorption of Mg-based mixtures elaborated by reactive mechanical grinding. *J. Alloys Comp.* 336, 292–296. doi: 10.1016/S0925-8388(01)01883-7

Bogdanović, B. (1984). Magnesium hydride: a homogeneous-catalysed synthesis and its use in hydrogen storage. *Int. J. Hydrog. Energ.* 9, 937–941. doi: 10.1016/0360-3199(84)90159-9

Bogdanović, B., Bohmhammel, K., Christ, B., Reiser, A., Schlichte, K., Vehlen, R., et al. (2010). Thermodynamic investigation of the magnesium–hydrogen system. *J. Alloys Compd.* 282, 84–92. doi: 10.1016/S0925-8388(98)00829-9

Chen, G., Zhang, Y., Chen, J., Guo, X., Zhu, Y., and Li, L. (2018). Enhancing hydrogen storage performances of MgH2 by Ni nano-particles over mesoporous carbon CMK-3. *Nanotechnology* 29:265705. doi: 10.1088/1361-6528/aabcf3

Ding, X., Ding, H., Song, Y., Xiang, C., Li, Y., and Zhang, Q. (2019). Activity-tuning of supported co–ni nanocatalysts via composition and morphology for hydrogen storage in MgH2. *Front. Chem.* 7:937. doi: 10.3389/fchem.2019.00937

Eleskandarany, M. S., Shabaan, E., Ali, N., Aldakheel, F., and Alkandary, A. (2016). *In-situ* catalyzation approach for enhancing the hydrogenation/dehydrogenation kinetics of MgH_2 powders with Ni particles. *Sci. Rep.* 6:37335. doi: 10.1038/srep37335

Gu, H., Zhu, Y., and Li, L. (2009). Hydrogen storage properties of Mg–Ni–Cu prepared by hydriding combustion synthesis and mechanical milling (HCS+MM). *Int. J. Hydrog. Energ.* 34, 2654–2660. doi: 10.1016/j.ijhydene.2009.01.068

Gulicovski, J., Rašković-Lovre, Ž., Kurko, S., Vujasin, R., Jovanović, Z., Matović, L., et al. (2012). Influence of vacant CeO2 nanostructured ceramics on MgH2 hydrogen desorption properties. *Ceram. Int.* 38, 1181–1186. doi: 10.1016/j.ceramint.2011.08.047

Hanada, N., Ichikawa, T., and Fujii, H. (2005). Catalytic effect of nanoparticle 3d-transition metals on hydrogen storage properties in magnesium hydride MgH2 prepared by mechanical milling. *J. Phys. Chem. B* 109, 7188–7194. doi: 10.1021/jp044576c

Hong, S-H., Kwon, S. N., Bae, J-S., and Song, M. Y. (2009). Hydrogen-storage properties of gravity cast and melt spun Mg-Ni-Nb_2O_5 alloys. *Int. J. Hydrog. Energ.* 34, 1944–1950. doi: 10.1016/j.ijhydene.2008.12.015

Jain, I. P., Lal, C., and Jain, A. (2010). Hydrogen storage in Mg: a most promising material. *Int. J. Hydrog. Energ.* 35, 5133–5144. doi: 10.1016/j.ijhydene.2009.08.088

Khan, D., Zou, J., Zeng, X., and Ding, W. (2018). Hydrogen storage properties of nanocrystalline Mg2Ni prepared from compressed 2MgH2Ni powder. *Int. J. Hydrog. Energ.* 43, 22391–22400. doi: 10.1016/j.ijhydene.2018.10.055

Kissinger, H. E. (1957). Reaction kinetics in differential thermal analysis. *Anal. Chem.* 29, 1702–1706.

Li, J., Li, B., Shao, H., Li, W., and Lin, H. (2018). Catalysis and downsizing in mg-based hydrogen storage materials. *Catalysts* 8:89. doi: 10.3390/catal8020089

Lin, H. -J., Matsuda, J., Li, H. -W., Zhu, M., and Akiba, E. (2015). Enhanced hydrogen desorption property of MgH2 with the addition of cerium fluorides. *J. Alloys Compd.* 645, S392–S396. doi: 10.1016/j.jallcom.2014.12.102

Lin, H. J., Ouyang, L. Z., Wang, H., Zhao, D. Q., Wang, W. H., Sun, D. L., et al. (2012a). Hydrogen storage properties of Mg–Ce–Ni nanocomposite induced from amorphous precursor with the highest Mg content. *Int. J. Hydrog. Energ.* 37, 14329–14335. doi: 10.1016/j.ijhydene.2012.07.073

Lin, H. -J., Tang, J. -J., Yu, Q., Wang, H., Ouyang, L. -Z., Zhao, Y. -J., et al. (2014). Symbiotic $CeH_{2.73}/CeO_2$ catalyst: a novel hydrogen pump. *Nano Energ.* 9, 80–87. doi: 10.1016/j.nanoen.2014.06.026

Lin, H. J., Wang, W. H., and Zhu, M. (2012b). Room temperature gaseous hydrogen storage properties of Mg-based metallic glasses with ultrahigh Mg contents. *J Non-Crystalline Solids* 358, 1387–1390. doi: 10.1016/j.jnoncrysol.2012.03.015

Lin, H. -J., Zhang, C., Wang, H., Ouyang, L., Zhu, Y., Li, L., et al. (2016). Controlling nanocrystallization and hydrogen storage property of Mg-based amorphous alloy via a gas-solid reaction. *J. Alloys Compd.* 685, 272–277. doi: 10.1016/j.jallcom.2016.05.286

Liu, Y., Du, H., Zhang, X., Yang, Y., Gao, M., and Pan, H. (2016). Superior catalytic activity derived from a two-dimensional Ti3 C2 precursor towards

the hydrogen storage reaction of magnesium hydride. *Chem. Commun.* 52, 705–708. doi: 10.1039/C5CC08801A

Liu, Y., Zhu, J., Liu, Z., Zhu, Y., Zhang, J., and Li, L. (2019). Magnesium nanoparticles with Pd decoration for hydrogen storage. *Front. Chem.* 7:949. doi: 10.3389/fchem.2019.00949

Long, S., Zou, J., Liu, Y., Zeng, X., and Ding, W. (2013). Hydrogen storage properties of a Mg–Ce oxide nano-composite prepared through arc plasma method. *J. Alloys Compd.* 580 (Suppl. 1), S167–S170. doi: 10.1016/j.jallcom.2013.02.063

Lototskyy, M., Sibanyoni, J. M., Denys, R. V., Williams, M., Pollet, B. G., and Yartys, V. A. (2013). Magnesium–carbon hydrogen storage hybrid materials produced by reactive ball milling in hydrogen. *Carbon* 57, 146–160. doi: 10.1016/j.carbon.2013.01.058

Ma, X., Xie, X., Liu, P., Xu, L., and Liu, T. (2017). Synergic catalytic effect of Ti hydride and Nb nanoparticles for improving hydrogenation and dehydrogenation kinetics of Mg-based nanocomposite. *Prog. Nat. Sci. Mater. Int.* 27, 99–104. doi: 10.1016/j.pnsc.2016.12.013

Mohtadi, R., and Orimo, S. -I. (2016). The renaissance of hydrides as energy materials. [Review Article]. *Nat. Rev. Mater.* 2:16091. doi: 10.1038/natrevmats.2016.91

Ouyang, L., Cao, Z., Wang, H., Hu, R., and Zhu, M. (2017). Application of dielectric barrier discharge plasma-assisted milling in energy storage materials – a review. *J. Alloys Compd.* 691, 422–435. doi: 10.1016/j.jallcom.2016.08.179

Ouyang, L., Cao, Z., Wang, H., Liu, J., Sun, D., Zhang, Q., et al. (2014b). Enhanced dehydriding thermodynamics and kinetics in Mg (In)–MgF2 composite directly synthesized by plasma milling. *J. Alloys Compd.* 586, 113–117. doi: 10.1016/j.jallcom.2013.10.029

Ouyang, L. Z., Cao, Z. J., Wang, H., Liu, J. W., Sun, D. L., Zhang, Q. A., et al. (2013). Dual-tuning effect of In on the thermodynamic and kinetic properties of Mg2Ni dehydrogenation. *Int. J. Hydrogen Energ.* 38, 8881–8887. doi: 10.1016/j.ijhydene.2013.05.027

Ouyang, L. Z., Yang, X. S., Zhu, M., Liu, J. W., Dong, H. W., Sun, D. L., et al. (2014a). enhanced hydrogen storage kinetics and stability by synergistic effects of *in situ* formed CeH2.73 and Ni in CeH2.73-MgH2-Ni nanocomposites. *J. Phys. Chem. C* 118, 7808–7820. doi: 10.1021/jp500439n

Reilly, J. J., and Wiswall, R. H. (1968). Reaction of hydrogen with alloys of magnesium and nickel and the formation of Mg_2NiH_4. *Inorg. Chem.* 7, 2254–2256. doi: 10.1021/ic50069a016

Rusman, N. A. A., and Dahari, M. (2016). A review on the current progress of metal hydrides material for solid-state hydrogen storage applications. *Int. J. Hydrog. Energ.* 41, 12108–12126. doi: 10.1016/j.ijhydene.2016.05.244

Shao, H., Felderhoff, M., Schüth, F., and Weidenthaler, C. (2011). Nanostructured Ti-catalyzed MgH2 for hydrogen storage. *Nanotechnology* 22:235401. doi: 10.1088/0957-4484/22/23/23540

Shao, H., He, L., Lin, H., and Li, H.-W. (2018). Progress and trends in magnesium-based materials for energy-storage research: a review. *Energ. Technol.* 6, 445–458. doi: 10.1002/ente.201700401

Shao, H., Xin, G., Zheng, J., Li, X., and Akiba, E. (2012). Nanotechnology in Mg-based materials for hydrogen storage. *Nano Energ.* 1, 590–601. doi: 10.1016/j.nanoen.2012.05.005

Terashita, N., Takahashi, M., Kobayashi, K., Sasai, T., Akiba, E. (1999). Synthesis and hydriding/dehydriding properties of amorphous Mg_2 $Ni_{1.9}$ $M_{0.1}$ alloys mechanically alloyed from $Mg_2Ni_{0.9}M_{0.1}$ (M=none, Ni, Ca, La, Y, Al, Si, Cu and Mn) and Ni powder. 5, 541–545.

Trovarelli, A. (1996). Catalytic properties of ceria and CeO2-containing materials. *Catalysis Rev.* 38, 439–520. doi: 10.1080/01614949608006464

Wang, H., Lin, H. J., Cai, W. T., Ouyang, L. Z., and Zhu, M. (2016). Tuning kinetics and thermodynamics of hydrogen storage in light metal element based systems – a review of recent progress. *J. Alloys Compds.* 658, 280–300. doi: 10.1016/j.jallcom.2015.10.090

Wang, Y., and Wang, Y. (2017). Recent advances in additive-enhanced magnesium hydride for hydrogen storage. *Prog. Nat. Sci. Mater. Int.* 27, 41–49. doi: 10.1016/j.pnsc.2016.12.016

Xu, C., Lin, H.-J., Wang, Y., Zhang, P., Meng, Y., Zhang, Y., et al. (2019). Catalytic effect of *in situ* formed nano-Mg2Ni and Mg2Cu on the hydrogen storage properties of Mg-Y hydride composites. *J. Alloys Compds.* 782, 242–250. doi: 10.1016/j.jallcom.2018.12.223

Zhan, L., Zhang, Y., Zhu, Y., Zhuang, X., Dong, J., Guo, X., et al. (2016). The electrochemical hydrogen storage properties of Mg67– xPdxCo33 (x= 1, 3, 5, 7) electrodes with BCC phase. *J. Alloys Compds.* 662, 396–403. doi: 10.1016/j.jallcom.2015.12.068

Zhang, J., Zhu, Y., Lin, H., Liu, Y., Zhang, Y., Li, S., et al. (2017). Metal hydride nanoparticles with ultrahigh structural stability and hydrogen storage activity derived from microencapsulated nanoconfinement. *Adv. Mater.* 29:1700760. doi: 10.1002/adma.201700760

Zhang, Y., Zhang, H., Ding, X., Liu, D., Zhang, Q., and Si, T. (2018). Microstructure characterization and hydrogen storage properties study of Mg2Ni0.92M0.08 (M = Ti, V, Fe or Si) alloys. *Prog. Nat. Sci. Mater. Int.* 28, 464–469. doi: 10.1016/j.pnsc.2018.06.006

Zhu, Y., Luo, S., Lin, H., Liu, Y., Zhu, Y., Zhang, Y., et al. (2017). Enhanced hydriding kinetics of Mg-10 at% Al composite by forming Al12 Mg17 during hydriding combustion synthesis. *J. Alloys Compd.* 712, 44–49. doi: 10.1016/j.jallcom.2017.04.049

Conflict of Interest: The authors declare that the research was conducted in the absence of any commercial or financial relationships that could be construed as a potential conflict of interest.